Journal of Neurochemistry

JOURNAL OF NEUROCHEMISTRY | 2015

doi: 10.1111/jnc.13230

ORIGINAL ARTICLE

Riluzole rescues glutamate alterations, cognitive deficits, and tau pathology associated with P301L tau expression

Holly C. Hunsberger,* Daniel S. Weitzner,* Carolyn C. Rudy,* James E. Hickman,* Eric M. Libell,† Rebecca R. Speer,† Greg A. Gerhardt‡ and Miranda N. Reed*,§,¶,**

*Behavioral Neuroscience, Department of Psychology, West Virginia University, Morgantown, West Virginia, USA

†Department of Biology, West Virginia University, Morgantown, West Virginia, USA

‡Center for Microelectrode Technology (CenMeT), Department of Anatomy and Neurobiology, University of Kentucky Health Sciences Center, Lexington, Kentucky, USA

§Center for Neuroscience, West Virginia University, Morgantown, West Virginia, USA

¶Center for Basic and Translational Stroke Research, West Virginia University, Morgantown, West Virginia, USA

**Drug Discovery & Development Department, School of Pharmacy, Auburn University, Auburn, Alabama

Abstract

Hyperexcitability of the hippocampus is a commonly observed phenomenon in the years preceding a diagnosis of Alzheimer's disease (AD). Our previous work suggests a dysregulation in glutamate neurotransmission may mediate this hyperexcitability, and glutamate dysregulation correlates with cognitive deficits in the rTg(TauP301L)4510 mouse model of AD. To determine whether improving glutamate regulation would attenuate cognitive deficits and AD-related pathology, TauP301L mice were treated with riluzole (~ 12.5 mg/kg/day p.o.), an FDA-approved drug for amyotrophic lateral sclerosis that lowers extracellular glutamate levels. Riluzole-treated TauP301L mice exhibited improved performance in the water radial arm maze and the Morris water maze, associated with a decrease in glutamate release and an increase in glutamate uptake in the dentate gyrus, cornu ammonis 3 (CA3), and cornu ammonis 1 (CA1) regions of the hippocampus. Riluzole also attenuated the TauP301L-mediated increase in hippocampal vesicular glutamate transporter 1, which packages glutamate into vesicles and influences glutamate release; and the TauP301L-mediated decrease in hippocampal glutamate transporter 1, the major transporter responsible for removing glutamate from the extracellular space. The TauP301L-mediated reduction in PSD-95 expression, a marker of excitatory synapses in the hippocampus, was also rescued by riluzole. Riluzole treatment reduced total levels of tau, as well as the pathological phosphorylation and conformational changes in tau associated with the P301L mutation. These findings open new opportunities for the development of clinically applicable therapeutic approaches to regulate glutamate in vulnerable circuits for those at risk for the development of AD.

Keywords: Alzheimer's disease, glutamate clearance, hippocampus, memory, riluzole, tau.

J. Neurochem. (2015) 10.1111/jnc.13230

Alzheimer's disease (AD) is a neurodegenerative disorder that targets vulnerable neural networks, particularly those involved in learning and memory (Palop *et al.* 2006; Brier

Received February 27, 2015; revised manuscript received June 22, 2015; accepted June 30, 2015.

Correspondence and present address: Miranda N. Reed, Auburn University, 4306 Walker Building, Auburn, AL 36849, USA. E-mail: reedmir@auburn.edu

Abbreviations used: AD, Alzheimer's disease; ALS, amyotrophic lateral sclerosis; AUC, area under the curve; Aβ, beta-amyloid; CA1, cornu ammonis 1; CA3, cornu ammonis 3; CaMKII, calcium/calmodulin kinase II; DG, dentate gyrus; DOX, doxycycline; GLT-1, glutamate transporter 1; GluOx, glutamate-oxidase; KCl, potassium chloride; MEA, microelectrode array; MWM, Morris water maze; PCI, platform crossing index; REF, reference; tTA, tetracycline-controlled transcriptional activation; vGLUT-1, vesicular glutamate transporter 1; WMC, working memory correct; WMI, working memory incorrect; WRAM, water radial arm maze.

et al. 2012). In the years preceding AD diagnosis, a hyperactivity of the distributed memory network is often observed in those at risk for AD (Bookheimer *et al.* 2000; Bondi *et al.* 2005; Bassett *et al.* 2006; Filippini *et al.* 2009; Quiroz *et al.* 2010; Sperling *et al.* 2010). Although originally this hyperactivity was believed to serve a compensatory function for deteriorating circuitry (Bondi *et al.* 2005), more recent evidence suggests this hyperactivity may be indicative of excitotoxicity, could directly contribute to cognitive impairment, and may even be permissive for the development of AD (Mackenzie and Miller 1994; Kamenetz *et al.* 2003; Busche *et al.* 2008, Koh *et al.* 2010; Bakker *et al.* 2012; Vossel *et al.* 2013; Yamada *et al.* 2014).

Using a tau mouse model of AD (rTg(TauP301L)4510), we recently showed (Hunsberger *et al.* 2014a) that P301L tau expression is associated with increased hippocampal glutamate release and decreased glutamate uptake, and these alterations in glutamate signaling correlated with cognitive deficits in the hippocampal-dependent Barnes maze task. The dysregulation of glutamate in mice expressing P301L tau was observed at a time when tau pathology was subtle and before readily detectable neuron loss. Here, we sought to determine whether reducing extracellular glutamate levels would alleviate cognitive deficits associated with P301L tau expression. To test this hypothesis, TauP301L mice were given riluzole, an FDA-approved disease-modifying drug for amyotrophic lateral sclerosis, that modulates glutamatergic signaling. At pharmacologically relevant drug concentrations, riluzole's *in vivo* mechanisms of action include a stabilization of the inactivate state of the voltage-gated sodium channel, leading to a decrease in glutamate release, and a potentiation of glutamate uptake via an increase in glutamate transporter expression (Azbill *et al.* 2000; Frizzo *et al.* 2004; Fumagalli *et al.* 2008; Gourley *et al.* 2012). Although other effects have been noted in *in vitro* studies, these effects only occur at unrealistically high concentrations, which are unlikely to be achieved in animals or patients (see Pittenger *et al.* 2008, for review).

We assessed the effects of riluzole administration on hippocampal-dependent learning and memory, glutamate regulation in the hippocampus [dentate gyrus (DG), cornu ammonis 3 (CA3), and cornu ammonis 1 (CA1)], and tau pathology in the hippocampus of TauP301L mice. Focus was given to the hippocampus because of its role in cognitive functions such as learning and memory, and because it is one of the first structures affected in AD (Braak and Braak 1998; Du *et al.* 2004; van de Pol *et al.* 2007). This increased vulnerability may be because of the high concentration of glutamate receptors that mediate communication of the trisynaptic circuit (DG, CA1, CA3) of the hippocampus (Greenamyre and Young 1989). Although the subregions of this circuit are connected, they differ in terms of synaptic connectivity, surface expression of glutamate receptors, gene expression profiles, and levels of glutamate release and clearance following evoked release (Gegelashvili and Schousboe 1998; Wilson *et al.* 2005b; Greene *et al.* 2009). For these reasons, we examined the subregions of the trisynaptic circuit separately. Riluzole's effects on glutamate regulation in these subregions were compared *in vivo* using microelectrode arrays (MEAs) coupled with amperometry. This is the first time riluzole's effects on glutamate have been examined using this approach, which allows for a high-resolution spatio-temporal study of the complex connections of the trisynaptic loop of the hippocampus *in vivo* without disrupting extrinsic and intrinsic connections. Results from our work suggest targeting excess hippocampal activity using riluzole may have therapeutic potential for the prevention of AD.

Materials and methods

Mice

Mice expressing P301L mutant human tau linked to a hereditary tauopathy were created by crossing mice harboring a responder transgene with mice harboring an activator transgene, as previously described (SantaCruz *et al.* 2005; Paulson *et al.* 2008). Briefly, activator mice (129s6 background strain) were crossed with responder mice (FVB/N background strain) to create regulatable transgenic mice expressing human four-repeat tau lacking the N-terminal sequences (4R0N) with the P301L mutation. To avoid mutant tau expression during the perinatal and early postnatal stages, 40 ppm doxycycline (DOX) hyclate was administered via water bottles to breeder dams for 3 weeks prior to mating and to all experimental mice from birth until 2.5 months of age (Hölscher 1999). All mice were housed, between two and five per cage, in a temperature and humidity-controlled colony room with a 12:12 light/dark cycle. All experimental procedures were conducted in accordance with the standards of International Animal Care and Use Committee, and the West Virginia University Animal Care and Use Committee approved all experimental procedures used in the study.

Experimental design

At 2.5 months of age, while still on DOX to suppress tau expression, mice underwent behavioral testing in the water radial arm maze (WRAM) to establish that cognitive deficits were dependent upon tau expression as previously described (Hunsberger *et al.* 2014b) (Fig. 1). After pre-tau behavioral testing, DOX was removed from the drinking water, and three groups of mice were established: Vehicle-Controls (N = 21; n = 10 female, n = 11 males), Vehicle-TauP301L (N = 24; n = 9 female, n = 15 males), and Riluzole-TauP301L (N = 19; n = 11 female, n = 8 males). TauP301L mice were randomly assigned to treatment groups (vehicle or riluzole) based on their home cage assignment. Pre-tau WRAM performance was assessed to ensure no pre-treatment differences were observed among the groups prior to starting treatment.

At 5 and 7.5 months of age, after 2.5 and 5 months of tau expression, respectively, mice underwent post-tau cognitive testing in the WRAM and Morris water maze (MWM). One male Vehicle-TauP301L male died during the course of the experiment, thus reducing the total sample size for the final round of behavioral testing at 7.5 months of age. WRAM and MWM testing were

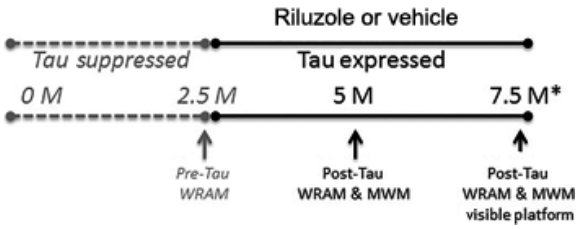

Fig. 1 Experimental design. Tau expression was suppressed from conception until 2.5 months (M) of age. Mice underwent testing in the water radial arm maze (WRAM) at 2.5 M of age, prior to the onset of tau expression. After WRAM testing at 2.5 M, tau expression began, and riluzole or vehicle was administered via the drinking water. Mice underwent behavioral testing at 5 and 7.5 M of age, after 2.5 and 5 M of tau expression, in the WRAM and Morris water maze (MWM). At the end of MWM testing at 7.5 M of age, the visible platform test was conducted to ensure no differences in visual or motoric function. At the end of visible platform testing, mice underwent anesthetized glutamate recordings (*).

separated by 1 day. Mice underwent visible platform training approximately 30 min after the last MWM probe trial at 7.5 months of age. Following behavioral testing, mice underwent *in vivo* anesthetized glutamate recordings and were killed immediately afterward.

Riluzole administration

Riluzole-TauP301L mice received riluzole (Sigma-Aldrich, St. Louis, MO, USA) + 1% *w/v* saccharin (vehicle) in the drinking water. Riluzole was dissolved by stirring the compound in ~ 23°C tap water, and solutions were changed every 72 h. Light-protectant water bottles were weighed daily, and the concentration of riluzole adjusted every 72 h such that intake remained at ~ 12.5 mg/kg/day (per os) for each cage, a dose previously tested in mice (e.g., Ishiyama *et al.* 2004; Gourley *et al.* 2012). The benefit of dissolving riluzole in the drinking water, rather than administering daily injections, is that this is a more robust and easily replicable administration protocol, administration via drinking water minimizes the stress associated with daily drug injections, and oral administration is the route riluzole is administered in humans. Vehicle-Controls and Vehicle-TauP301L mice consumed saccharin (vehicle) alone. All animals received food *ad libitum*.

Riluzole has a good pharmacokinetic profile (Wagner and Landis 1997), including an absorption of 90% following oral administration, a bioavailability of 60%, peak concentrations within 1–1.5 h, a 12 h half-life, and minor side effects. The most commonly reported adverse effects in humans include nausea and asthenia (Miller *et al.* 2003). The dose used here (12.5 mg/kg/day) was chosen because previous research using mice administered riluzole via their drinking water suggests this dose increases glutamate glial transporter 1 (GLT-1) expression without significantly affecting baseline locomotor activity, thymus and adrenal gland weights, or blood serum corticosterone (Gourley *et al.* 2012). Similarly, we observed no differences in water consumption or bodyweight among the treatment Groups at 5 or 7.5 months of age (*p*s > 0.1), and swim speeds in the MWM did not differ at 5 or 7.5 months of age (*p*s > 0.1), suggesting this dose of riluzole was not toxic and did not produce nausea or asthenia.

Water radial arm maze

The WRAM was performed as previously described (Bimonte-Nelson *et al.* 2003). The maze was filled with water at 22°C and made opaque with non-toxic white paint. Four of the eight arms contained hidden platforms (8 × 8 cm) with wire mesh tops located 1 cm below the surface of the water. The location of the platforms were counter-balanced across the groups, but remained fixed for a particular mouse for the duration of testing at a particular age. A platform was never in more than two adjacent arms or in the 'start arm' from which a mouse was released. Salient extra-maze cues remained constant for the duration of testing at a particular age. However, both the location of the platform arms and the cues were changed at subsequent ages.

Once released from the start arm, the mouse had 2 min to locate a hidden platform. If the allotted time expired, the mouse was guided to the nearest platform. Once a platform was found, the mouse remained on the platform for 15 s. At that point, the mouse was removed and placed in the holding cage lined with paper towels and warmed to ~ 31°C by a heating pad and heat lamp for 30 s to prevent hypothermia. During the interval, the just-chosen platform was removed. Each mouse was given four trials per session and one session per day. One platform was removed after each trial until only one platform remained in trial 4. Thus, each subsequent trial resulted in an increase in memory load, as the mice had to remember not only the locations of the remaining platforms, but also the platforms that had already been found (Bimonte-Nelson *et al.* 2003).

Each mouse was given 1 session a day for 11 consecutive days. Day 1 was considered a training session because the mice did not have previous experience in the maze, whereas days 2–11 were considered learning trials for acquisition (Bimonte-Nelson *et al.* 2003). On day 12, a 4-h delay was inserted between trials 2 and 3. On day 13, a 6-h delay was inserted between trials 2 and 3. Delays were inserted to increase memory demand for the trials following the delay (Engler-Chiurazzi *et al.* 2011).

An arm entry was defined as all four paws entering into an arm of the maze. Reference memory (REF) errors were defined as the number of first entries into any arm that never contained a platform. Working memory incorrect (WMI) errors were defined as the number of repeat entries into an arm that never contained a platform (i.e., repeat entries into a reference memory arm). Working memory correct (WMC) errors were defined as the number of first and repeat entries into any arm where a platform had been during a previous trial. Errors were analyzed for each daily session for days 2–11. For days 12 and 13, the average number of errors on trials after the delay (trials 3 and 4) was analyzed.

Morris water maze

The MWM was performed as previously described (Zhang *et al.* 2008). Briefly, at 5 months of age, each mouse received 4 days of total testing (6 trials × 2 days + 4 trials × 1 day + 1 probe × 1 day). Spatial learning was examined in the MWM with hidden platform. During hidden platform training, the pool was filled with water at 22°C. A platform was hidden 1 cm under the opaque water in one of four quadrants. During hidden platform training (Days 1–3), the mouse was released from predetermined, semi-random starting locations, and swam for either 60 s, or until it reached a hidden platform. Once on the platform for 15 s, the mouse was removed and placed in the holding cage lined with paper towels

and warmed to ~31°C. The intertrial interval was 20 min. For hidden platform training, pathlength was compared. On Day 4, a probe trial, where the platform was removed, was conducted, and the platform crossing index (PCI) and percent time in the target quadrant were recorded during the 60-s test. A second probe trial was conducted 24 h later. Salient extra-maze cues remained constant for the duration of testing at a particular age. However, both the location of the platform and the cues were changed at 7.5 months of age.

The initial training at 7.5 months of age was the same as that at 5 months of age (6 trials × 2 days + 4 trials × 1 day), but additional training and probe trials were conducted to determine if further training might reveal greater differences among the Groups. After the probe trial on Day 4, four additional training trials occurred. On Days 5 and 6, a probe trail was conducted followed by four training trials. On Day 7, each mouse underwent four training trials without a probe trial. On Day eight, the last day of MWM testing, each mouse underwent a probe trial only (Hunsberger *et al.* 2014b). Two mice (one Ril-TauP301L and one Veh-Control) were identified as outliers owing to an average hidden pathlength and swim speeds greater than two standard deviations above their group means; these mice were removed from MWM analyses.

Visible platform test

To ensure any deficits observed in the WRAM or MWM were not because of visual or motor deficits, the visible platform test was performed as previously described (Bimonte-Nelson *et al.* 2003) at the end of MWM testing at 7.5 months of age. A black platform with a flag raised was placed approximately 2.5 cm above the water level. Each mouse was placed into the tub facing the wall opposite the platform and given 2 min to swim to the platform. If the mouse found the platform within the allotted time limit, the mouse remained on the platform for 20 s; if the mouse did not find the platform, the mouse was gently guided to the platform. After each mouse completed the first trial, the platform was moved to a new location along the back wall of the tub. All mice were given five independent trials with approximately 10 min between each trial.

Enzyme-based microelectrode arrays

Ceramic-based MEAs, consisting of a ceramic-based multisite microelectrode with four platinum recording sites (Burmeister and Gerhardt 2001), were used to examine glutamate regulation and were purchased from Quanteon, L.L.C. (Nicholasville, KY, USA) as previously described (Hunsberger *et al.* 2014a). Briefly, recording sites were covered with glutamate-oxidase to oxidize glutamate to alpha-ketoglutarate and hydrogen peroxide (H_2O_2), the reporter molecule (Burmeister and Gerhardt 2001). The background current from the sentinel sites was then subtracted from the recording sites to produce a selective measure of extracellular glutamate. Calibrations were conducted on the MEAs prior to their use. Using the FAST-16 mkII system (Quanteon, L.L.C.), a constant potential of +0.7 V versus an Ag/AgCl reference was applied to the MEA to oxidize the reporter molecule. The MEA tip was submerged in 40 mL of a 0.05 M phosphate-buffered saline maintained at 37°C. Ascorbic acid (250 μM) and dopamine (2 μM) were added to the solution to determine selectivity for glutamate (Hinzman *et al.* 2012). A standard curve was determined by adding successive aliquots of glutamate.

For intracranial drug deliveries, a glass micropipette with an inner diameter tip of 10–15 μm (Quanteon, L.L.C.) was centered between the recording pairs and positioned 80–100 μm away from the MEA surface. The micropipette was attached to a Picospritzer III (Parker-Hannifin, Cleveland, OH, USA) and set to consistently deliver volumes of 50–100 nL of sterile-filtered isotonic 70 mM KCl solution or 200 μM glutamate solution at a pressure of 0.138–1.38 bar for .30–2.5 s. Volume displacement was monitored using a stereomicroscope fitted with a reticule (Friedemann and Gerhardt 1992).

In vivo anesthetized recordings

Mice were anesthetized with isoflurane (1–4% inhalation; continuous) and placed into a stereotaxic apparatus. A rectal probe and a water pad connected to a recirculating water bath were used to ensure mice did not become hypothermic while under anesthesia. The MEA/micropipette array was placed into the DG, CA3, and CA1 of the hippocampus (Hunsberger *et al.* 2014a). Stereotaxic coordinates for the different subregions of the hippocampus were calculated using the mouse brain atlas (Paxinos and Franklin 2012) [DG (AP: −2.3 mm, ML: +/−1.5 mm, DV: 2.1 mm), CA3 (AP: −2.3 mm, ML: +/−2.7 mm, DV: 2.25 mm), CA1 (AP: −2.3 mm, ML: +/−1.7 mm, DV: 1.4 mm)]. Prior studies have shown that the MEAs produce minimal effects both acutely and chronically (Hascup *et al.* 2009). To confirm the stereotaxic coordinates targeted the regions of interest, an MEA with an attached micropipette was used to locally apply Fluoro-Ruby (Millipore, Bedford, MA, USA), and MEA placement following brain sectioning was confirmed, as previously shown (Hunsberger *et al.* 2014a). However, because brain tissue was used for immunoblotting, the MEA placement was not confirmed for each mouse.

All MEA recordings were performed at 10 Hz using constant potential amperometry. After the MEA reached a stable baseline (10–20 min), tonic glutamate levels (μM) were calculated by averaging extracellular glutamate levels over 10 s prior to any application of solutions. Evoked release (amplitude) was measured by local application of KCl delivered every 2–3 min in all three subregions of one hemisphere. Highly reproducible KCl-evoked release of glutamate is indicative of the intact glutamate neuronal system that is detected by the MEAs (Day *et al.* 2006). Results of 10 reproducible signals were averaged for each group, and the average amplitude compared (Nickell *et al.* 2007; Hinzman *et al.* 2010, 2012). KCl-evoked release of glutamate allowed for measurement of the 'capacity' or 'ceiling' of the nerve terminals to release glutamate (Hinzman *et al.* 2010).

Exogenous glutamate (200 μM) was applied every 2–3 min in the opposite hemisphere to examine glutamate uptake after the MEA reached a stable baseline (10–20 min). The net area under the curve (AUC) was used as a measure of glutamate uptake. Both the hemispheres used for KCl and glutamate application and the order of subregions within a hemisphere were counter-balanced. Data from some hippocampal regions were excluded for reasons including death during surgery, failure of the MEA, or clogging of the micropipette. For each glutamate-related measure, the number of mice per treatment group is indicated in the corresponding figure caption.

Immunoblotting

Immunoblotting steps have been described in detail previously (Hunsberger *et al.* 2014a). Briefly, protein concentrations of

hippocampal tissue were determined with a bicinchoninic acid protein assay. Hippocampal tissue samples were either heated to 70°C (vesicular glutamate transporter 1, vGLUT1 and synaptophysin) or 95°C (for all other proteins) for 5 min and then separated on 10% criterion gels (Bio-Rad Laboratories, Hercules, CA, USA), and transferred onto 0.45 μm polyvinylidene difluoride membranes (Millipore). Membrane blots were blocked for 1 h at ~ 23°C in 5% bovine serum albumin in 0.1% Tween 20/Tris-buffered saline (TTBS) or 5% milk in TTBS. After blocking, membranes were incubated with an antibody directed against the protein of interest overnight at 4°C. Membranes were incubated with the appropriate biotinylated or horseradish peroxidase-conjugated secondary antibody for 1.5 h at ~ 23°C. Blots were then incubated with SuperSignal West Pico chemiluminescent substrate (Thermo Scientific, Waltham, MA, USA) or Novex AP chemiluminescent substrate (Invitrogen, Carlsbad, CA, USA) for 5 min, and visualized using Fluorchem E imager (Cell Biosciences, Heidelberg, Vic). Membranes were stripped for 15 min with Restore PLUS western blot stripping buffer (Pierce, Rockford, IL, USA) and re-probed and normalized to synaptophysin or actin. Band density was measured using AlphaView software (Proteinsimple, Santa Clara, CA, USA).

Data analysis

As previously described (Hunsberger *et al.* 2014a), amperometric data were analyzed using a custom Microsoft excel software program (MatLab, Natick, MA, USA). Background current from the sentinel sites was subtracted from the signal obtained from the glutamate-oxidase recording sites to determine concentrations of glutamate in the hippocampus. The resting current (pA) was divided by the slope (μM/pA) obtained during calibration and reported as a concentration of glutamate.

All statistical analyses were performed using JMP (SAS, Cary, NC, USA). Statistical analysis consisted of ANOVA and repeated-measures ANOVA (RMANOVA). For all measures, the main effects of Group (Veh-Controls, Veh-P301L, Ril-P301L) and Sex (male, female), as well as the interaction between the two (Group × Sex) were assessed. For the RMANOVA of behavioral data, Trial or Probe served as the within-subject variables. All significant omnibus tests were followed by Tukey *post hoc* comparisons. Using Pearson r correlations, tonic glutamate, KCl-evoked glutamate release (amplitude), and glutamate uptake (net AUC) in the DG, CA3, and CA1 were correlated separately with performance in the MWM.

The critical alpha level was set to 0.05, and all values in the text and figures represent means ± SEM. Unless otherwise noted, there were no differences between the sexes and no Group × Sex interactions, and thus, focus is given to the effect of Group.

Results

Riluzole rescues cognitive deficits in TauP301L Mice

Pre-Tau WRAM performance

At 2.5 months of age, prior to the onset of tau expression, mice underwent WRAM testing to ensure no pre-tau differences in behavior and to assign TauP301L mice to treatment (riluzole or vehicle) groups. For acquisition, there was a within-subject effect of Trial for all three dependent measures, i.e., reference memory errors (REF), WMI, or WMC, but no main effects of Group, Sex, or Group × Sex interactions, nor any interactions with Trial (ps > 0.1; Figure S1a–c), suggesting similar acquisition across the groups. Similarly, during delay trials, there were no main effects of Group, Sex, or Group × Sex interactions for REF, WMI, or WMC (ps > 0.1; Figure S1d), indicating similar performance prior to tau expression.

Post-tau WRAM acquisition

At 5 and 7.5 months of age, after assignment to either vehicle or riluzole treatment and 2.5 and 5 months of tau expression, respectively, mice were again tested in the WRAM with new extra-maze cues and a reassignment of arms containing platforms at each age. During acquisition at 5 months of age, there was a main effect of Sex for REF [$F(1, 58) = 5.86$, $p = 0.02$], WMI [$F(1, 58) = 5.10$, $p = 0.03$], and WMC [$F(1, 58) = 4.21$, $p = 0.04$], such that females performed significantly better than males (Figure S2). These Sex effects were not driven by the Veh-TauP301L group, as no Sex differences were observed when the Veh-TauP301L group was analyzed separately (REF [$F(1, 22) = 2.03$, $p = 0.17$], WMI [$F(1, 22) = 0.93$, $p = 0.34$], and WMC [$F(1, 22) = 0.0006$, $p = 0.98$]). There was not a main effect of Group or a Group × Sex interaction, or any interactions with Trial, for any measure (ps > 0.1), suggesting similar acquisition (Figure 3a–c). When mice underwent testing again at 7.5 months of age, acquisition was similar across the groups, including the sexes, for all measures (ps > 0.1; Figure S3d–f).

Post-tau WRAM delay trials

To increase memory demand, a 4-h or 6-h delay was inserted between Trials 2 and 3 on Day 12 and 13, respectively. Memory retention for the post-delay trials (Trials 3 and 4) within that day was assessed, as previously described (Braden *et al.* 2010; Engler-Chiurazzi *et al.* 2011). We observed no impairing effects of the 4-h delay among the groups for any error measure at either age (ps > 0.1; Figure S4). However, insertion of a longer delay (6-h) between Trials 2 and 3 on Day 13 revealed impaired performance for WMI in Veh-TauP301L mice at 5 [$F(2, 58) = 4.18$, $p = 0.02$] and 7.5 [$F(2, 57) = 3.19$, $p = 0.05$] months of age, an effect rescued by riluzole treatment (Fig. 2).

Morris water maze

Swim speed did not differ among the groups at any age tested (ps > 0.1; Figure S5a and b), suggesting similar motoric functioning. At 5 months of age, Veh-TauP301L mice exhibited significantly longer pathlengths to the hidden platform during learning trials [Group: $F(2, 56) = 3.72$, $p = 0.03$; Fig. 3a]. Pathlength was similar across the groups for Trial 1 of Day 1 [$F(2, 56) = 0.378$, $p = 0.69$], suggesting differences in acquisition were not because of deficits in

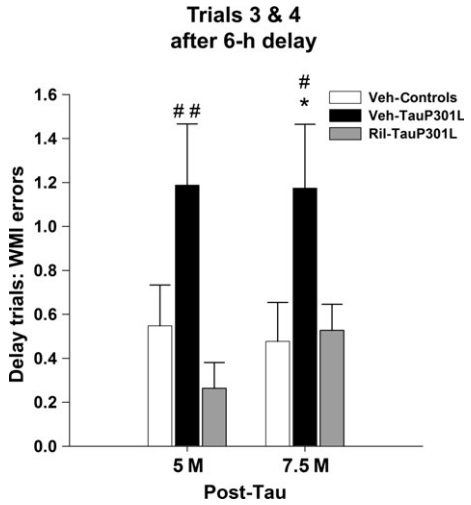

Fig. 2 Riluzole rescues cognitive deficits associated with P301L tau expression in the water radial arm maze (WRAM). Following the insertion of a 6-h delay between trials 2 and 3, TauP301L mice exhibited significantly more working memory incorrect (WMI) errors at 5 and 7.5 months (M) of age, an effect attenuated by riluzole treatment. (Mean ± SEM; $*p < 0.05$ Veh-Controls vs. Veh-TauP301L, $^{\#}p < 0.05$ Ril-TauP301L vs.Veh-TauP301L, $^{\#\#}p < 0.01$ Ril-TauP301L vs. Veh-TauP301L).

motoric functioning but rather learning. For the two probe trials employed at 5 months, there were no differences among the groups for the percent time in the target quadrant [$F(2, 56) = 0.84$, $p = 0.44$] or the PCI [$F(2, 56) = 0.66$, $p = 0.52$] (Figure S5c and d).

At 7.5 months of age, similar pathlengths were observed on Day 1 Trial 1 [$F(2, 55) = 0.19$, $p = 0.83$], indicating that prior to training, performance was similar among the groups. With additional training, comparison of the pathlength to the hidden platform revealed a between-subject effect of Group; the average hidden pathlength for Veh-TauP301L mice was significantly longer than that of Veh-Controls and Ril-TauP301L mice during learning trials [$F(2, 55) = 5.48$, $p = 0.007$; Fig. 3b]. Analysis of spatial reference memory during the four probe trials employed at 7.5 months of age revealed a significant main effect of Group for the percent time in the target quadrant [$F(2, 55) = 3.33$, $p = 0.04$; Fig. 3c], as well as the PCI [$F(2, 55) = 3.54$, $p = 0.04$; Fig. 3d]; riluzole improved probe trial performance in TauP301L mice.

Visible platform

To determine whether visual or motor deficits were present in any mice, thus affecting the results and interpretations of

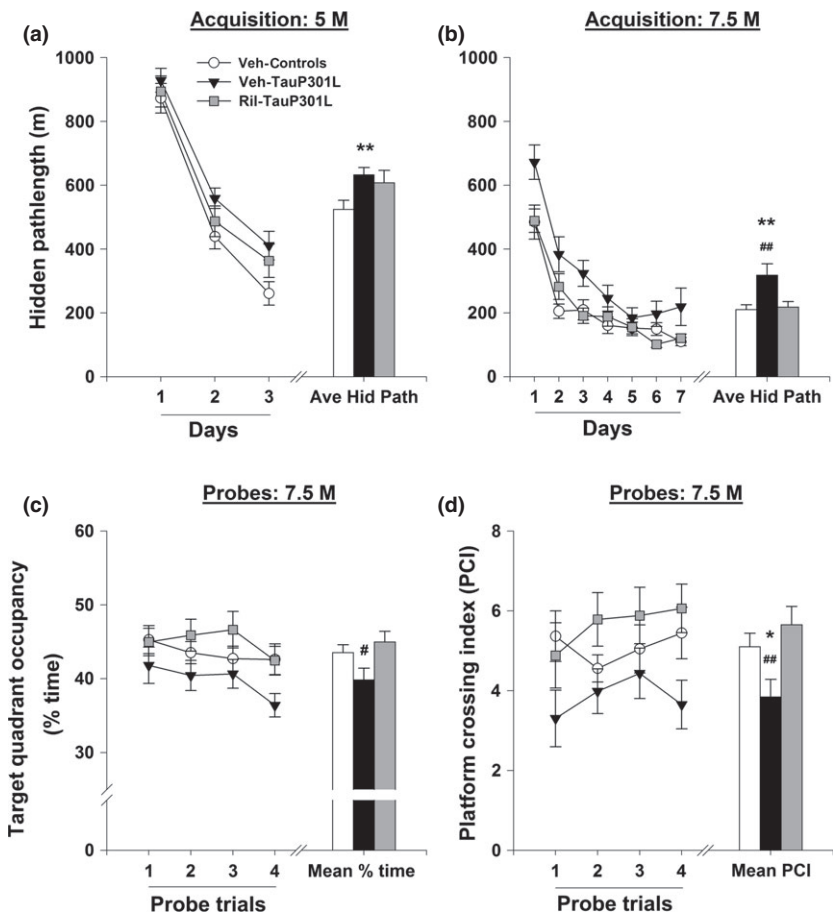

Fig. 3 Riluzole improves performance of TauP301L mice in the Morris water maze (MWM). Veh-TauP301L mice exhibited longer pathlengths during hidden platform training at 5 (a) and 7.5 (b) months of age. At 7.5 months of age, riluzole treatment rescued the deficits in spatial reference memory, as indicated by an increase in time spent in the target quadrant (c) and the PCI (d). Ave Hid Path, Average hidden pathlength; M, Months; PIC, platform crossing index. (Mean ± SEM; $*p < 0.05$ Veh-Controls vs. Veh-TauP301L, $**p < 0.01$ Veh-Controls vs. Veh-TauP301L, $^{\#}p < 0.05$ Ril-TauP301L vs.Veh-TauP301L, $^{\#\#}p < 0.01$ Ril-TauP301L vs.Veh-TauP301L).

behavioral testing, visible platform training was performed at the conclusion of WRAM and MWM behavioral testing. The average time to locate the visible platform did not differ among groups [Group: $F(2, 55) = 1.92$, $p = 0.16$; Sex: $F(1, 55) = 1.33$, $p = 0.25$; Group × Sex: $F(2, 55) = 2.45$, $p = 0.10$], suggesting similar orientation, visual, and motoric functioning (Figure S5e).

Riluzole rescues glutamate alterations in TauP301L mice

Tonic glutamate levels were not significantly different in the DG [$F(2, 44) = 1.53$; $p = 0.23$] among the groups. However, in the CA3 [$F(2, 47) = 3.42$; $p = 0.04$] and CA1 [$F(2, 47) = 8.29$; $p < 0.001$] regions, Veh-TauP301L mice exhibited increased tonic glutamate levels, an effect rescued by riluzole treatment (Fig. 4a). To examine the capacity for glutamate release, local application of 50–100 nL of 70 mM KCl was delivered via a micropipette and produced reproducible glutamate release in all regions of the hippocampus (Fig. 4b). The amplitudes of KCL-evoked-glutamate release were significantly increased in Veh-TauP301L mice in the DG [$F(2, 44) = 5.60$; $p = 0.007$], CA3 [$F(2, 46) = 13.49$; $p < 0.0001$] and CA1 [$F(2, 44) = 5.64$, $p = 0.007$]. Riluzole treatment rescued the P301L-mediated increase in KCl-evoked glutamate release in all three subregions (Fig. 4c).

Although glutamate clearance can be examined following KCl-evoked release of glutamate, KCl causes a non-selective release of neurotransmitters, including GABA, and has effects on glutamate transporter functioning. By applying physiologically relevant concentrations of exogenous glutamate, we can isolate glutamate clearance mechanisms and examine glutamate uptake *in vivo*. To confirm differences in net AUC among the groups following application of exogenous glutamate were because of alterations in uptake and not differences in the amount of glutamate applied, we first compared the amplitude of glutamate signals following administration of exogenous glutamate; no differences in amplitude were observed among the mice in the DG [$F(2, 37) = 2.57$; $p = 0.09$], CA3 [$F(2, 40) = 0.55$; $p = 0.58$], and CA1 [$F(2, 41) = 2.77$; $p = 0.08$] (Fig. 5a), suggesting similar applications of exogenous glutamate. To ensure no differences in the diffusion of glutamate in the extracellular space, we next compared Trise, the time for the signal to reach maximum amplitude, and found no differences among the groups in the DG [$F(2, 37) = 1.21$; $p = 0.31$], CA3 [$F(2, 40) = 1.55$; $p = 0.23$], and CA1 [$F(2, 41) = 1.54$; $p = 0.23$] (Fig. 5b), suggesting any reductions in glutamate uptake were not because of diffusion from the point source (micropipette) to the MEA (Sykova *et al.* 1998). The lack of differences in amplitude and Trise among the groups suggests any differences in net AUC likely results from decreases in glutamate uptake. Following exogenous application of glutamate, Veh-TauP301L mice exhibited an increased net AUC in the DG [$F(2, 37) = 6.49$, $p = 0.004$], CA3 [$F(2, 40) = 7.63$; $p = 0.0016$], and CA1 [$F(2, 41) = 4.23$; $p = 0.02$], suggesting reduced glutamate uptake in all three subregions of the hippocampus. Riluzole treatment improved glutamate uptake in all three regions (Fig. 5c and d).

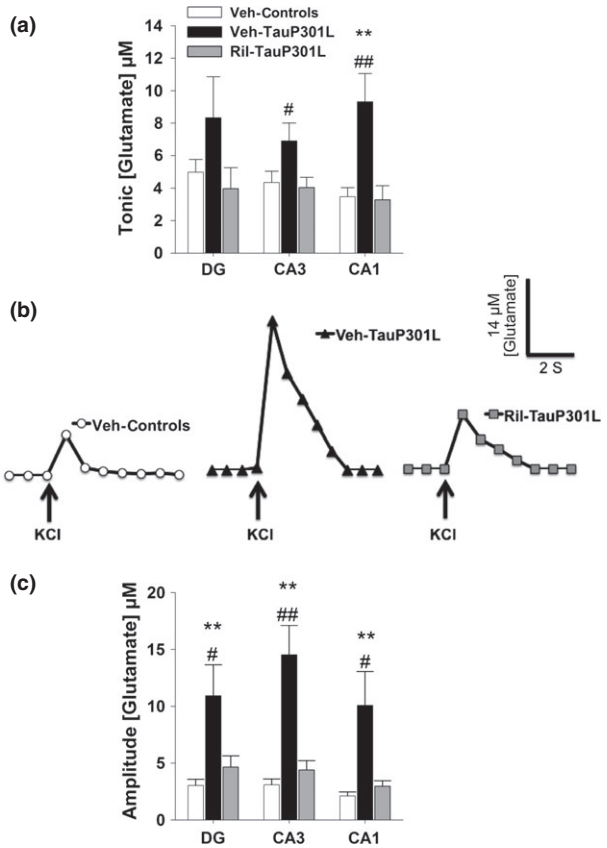

Fig. 4 Extracellular tonic and potassium chloride (KCl)-evoked release of glutamate in the dentate gyrus (DG), cornu ammonis 3 (CA3), and cornu ammonis 1 (CA1) regions of the hippocampus. (a) In the CA3 and CA1 regions of the hippocampus, tonic glutamate levels were significantly increased in Veh-TauP301L mice, an effect attenuated by riluzole treatment. (b) Baseline-matched representative recordings of KCl-evoked glutamate release in the CA3 showed riluzole treatment attenuated the significant increase in the amplitude of glutamate release observed in Veh-TauP301L mice. Local application of KCl (↑) produced a robust increase in extracellular glutamate that rapidly returned to tonic levels. (c) The significantly increased KCl-evoked glutamate release observed in Veh-TauP301L mice in the DG, CA3, and CA1 after local application of KCl was attenuated with riluzole treatment. (Mean ± SEM; $^{**}p < 0.01$ Veh-Controls vs. Veh-TauP301L, $^{\#}p < 0.05$ Ril-Tau3P01L vs.Veh-TauP301L, $^{\#\#}p < 0.01$ Ril-Tau3P01L vs.Veh-TauP301L; $n = 14$–19/group).

Glutamate alterations correlate with cognitive deficits in TauP301L mice

To determine whether glutamate (baseline, evoked release, and clearance) correlated with cognitive performance at 7.5 months of age, we first identified the behavioral outcome most sensitive to P301L tau expression. Calculating the effect size, we determined that the average hidden pathlength

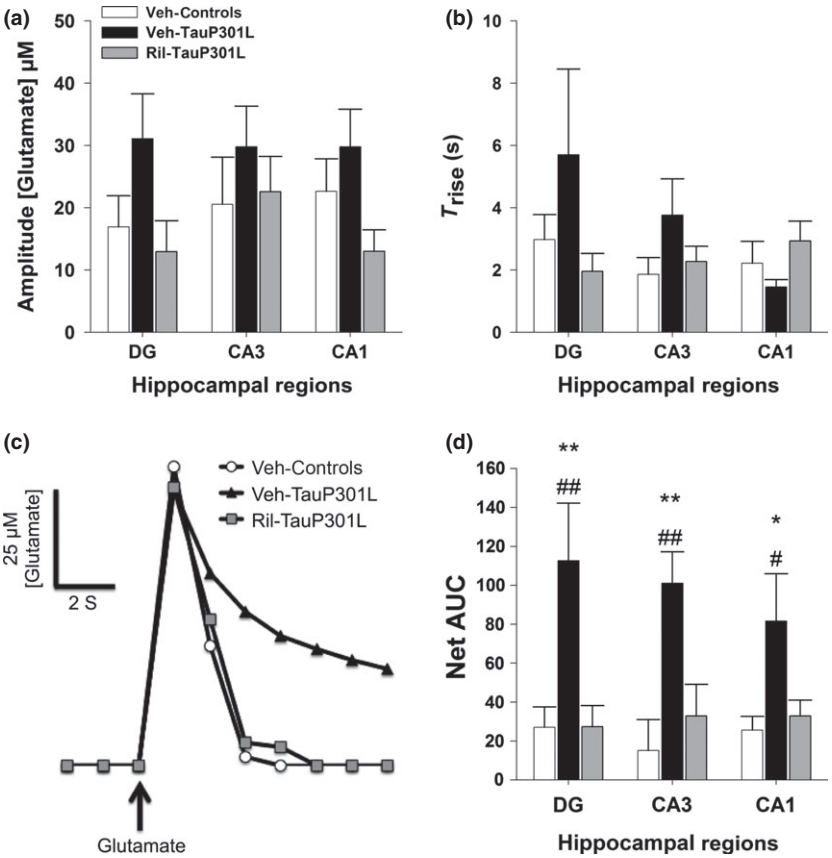

Fig. 5 Glutamate uptake following exogenous glutamate application in the dentate gyrus (DG), cornu ammonis 3 (CA3), and cornu ammonis 1 (CA1) regions of the hippocampus. (a) The amplitude of glutamate signal was similar among groups in each region. (b) Trise, an indicator of glutamate diffusion, was similar among the groups in each region. (c) Representative glutamate signals in the CA3 from local application of glutamate in Veh-Controls, Veh-TauP301L, and Ril-TauP301L mice. (d) Riluzole treatment reduced the significant increases in the net area under the curve (AUC) observed in Veh-TauP301L mice in all three regions of the hippocampus, indicating improved glutamate uptake in riluzole-treated TauP301L mice. (Mean ± SEM; $^{*}p < 0.05$ Veh-Controls vs. Veh-TauP301L, $^{**}p < 0.01$ Veh-Controls vs. Veh-TauP301L, $^{\#}p < 0.05$ Ril-TauP301L vs. Veh-TauP301L, $^{\#\#}p < 0.01$ Ril-TauP301L vs.Veh-TauP301L; n = 13–15/group).

in the MWM was the most sensitive measure of learning ($\eta^2 = 0.16$) and PCI was the most sensitive measure of memory ($\eta^2 = 0.15$) (Lipp and Wolfer 1998; Jeltsch *et al.* 2001) compared with percent time in the target quadrant in the MWM ($\eta^2 = 0.11$) and WMI errors in the WRAM ($\eta^2 = 0.09$).

The average hidden pathlength during learning trials was significantly correlated with tonic glutamate levels in the CA3 ($p = 0.0025$) and CA1 ($p = 0.023$) but not the DG ($p = 0.08$) of TauP301L mice (Table 1). As previously reported (Hunsberger *et al.* 2014a), performance was significantly correlated with glutamate uptake (net AUC) in the DG ($p = 0.028$) and CA1 ($p = 0.0056$) but not the CA3 ($p = 0.22$), while the opposite pattern was observed for amplitude of evoked glutamate release. KCl-evoked release in the CA3 was significantly correlated with MWM performance ($p = 0.0116$), whereas for the DG and CA1 regions, there was no relationship between release and performance ($p = 0.68$ and $p = 0.22$, respectively). Although swim speed did not differ among the groups during learning trials ($ps > 0.1$; Figure S5a and b), we nevertheless ran correlations between pathlength and swim speed to determine if the two were related. The correlation between pathlength and swim speed was not significant ($p = 0.28$). In addition, swim speed did not correlate with tonic, KCl-evoked release, or uptake in the DG, CA3, or CA1 ($ps > 0.1$), suggesting the relations among pathlength and glutamate signaling were because of differences in learning and not motoric functioning.

To assess the relations among memory and glutamate regulation, correlations between PCI during probe trials in the MWM and glutamate measures were conducted (Table 1). PCI during probe trials was significantly correlated with tonic glutamate levels in the DG ($p = 0.0016$), CA3 ($p = 0.02$), and CA1 ($p < 0.0001$) of TauP301L mice. In contrast to the pattern of relations observed between learning (i.e., pathlength) and KCl-evoked release and uptake, there were no significant relations between memory (PCI) and KCl-evoked release or clearance ($ps > 0.1$; Table 1).

Riluzole rectifies alterations of the tripartite synapse

As previously reported (Hunsberger *et al.* 2014a), hippocampal vGLUT1 expression was significantly increased in Veh-TauP301L mice [$F(2, 35) = 9.09$; $p = 0.0007$], an effect rescued by riluzole treatment (Fig. 6a). This difference in vGLUT1 expression was not because of a widespread increase in pre-synaptic terminals, as indicated by similar synaptophysin expression among the groups [$F(2, 35) = 0.19$; $p = 0.82$]. Riluzole treatment also increased

the P301L-mediated decrease in GLT-1 expression previously observed in TauP301L mice [$F(2, 35) = 8.37$, $p = 0.0011$; Fig. 6b]. There were no differences among the groups for the loading control, beta-actin [$F(2, 35) = 2.29$, $p = 0.12$]. PSD-95, a major post-synaptic scaffold protein at excitatory synapses, was used as a marker of excitatory synapses in the hippocampus. Riluzole treatment rescued the reduction in PSD-95 expression observed in Veh-TauP301L mice ([$F(2, 35) = 5.32$, $p = 0.01$]; Fig. 6c).

Riluzole attenuates tau pathology

We next determined whether riluzole treatment could attenuate tau pathology. Early changes in tau were examined using CP-13 and MC-1, which detect phosphorylation (pSer202) and conformation-specific changes, respectively. Both hippocampal CP-13 [$F(2, 34) = 25.72$, $p < 0.0001$] and MC-1 [$F(2, 35) = 113.95$, $p < 0.0001$] were increased in Veh-TauP301L mice. Riluzole treatment significantly decreased the immunoreactive signal for tau

Table 1 Correlations between glutamate dysregulation & learning acquisition (average hidden pathlength) and memory (PCI) in the Morris water maze for Veh-TauP301L mice (significant *p*-values in bold)

	DG	CA3	CA1
Tonic vs. Pathlength	Path = 278 + 3.4*Tonic $r^2(19) = 0.17$, $p = 0.08$	Path = 237 + 4.7*Tonic $r^2(19) = 0.43$, **$p = 0.0025$**	Path = 237 + 6.7*Tonic $r^2(19) = 0.27$, **$p = 0.0231$**
KCl-evoked Release vs. Pathlength	Path = 315 + 1.3*Amp $r^2(18) = 0.01$, $p = 0.68$	Path = 253 + 3.1*Amp $r^2(18) = 0.64$, **$p = 0.0116$**	Path = 263 + 4.1*Amp $r^2(17) = 0.10$, $p = 0.22$
Clearance vs. Pathlength	Path = 248 + 37*AUC $r^2(14) = 0.34$, **$p = 0.028$**	Path = 259 + 27*AUC $r^2(14) = 0.12$, $p = 0.22$	Path = 231 + 43*AUC $r^2(14) = 0.49$, **$p = 0.0056$**
Tonic vs. PCI	Path = 4.8–0.06*Tonic r^2 (19) = 0.45, **$p = 0.0016$**	Path = 4.6–0.05*Tonic r^2 (19) = 0.27, **$p = 0.0227$**	Path = 5.5–0.12*Tonic r^2 (19) = 0.61, **$p < 0.0001$**
KCl-evoked Release vs. PCI	Path = 4.1–0.006*Amp r^2 (18) = 0.001, $p = 0.88$	Path = 4.15–0.02*Amp r^2 (18) = 0.06, $p = 0.29$	Path = 4.22–0.005*Amp r^2 (17) = 0.001, $p = 0.91$
Clearance vs. PCI	Path = 4.5–0.0003*AUC $r^2(14) = 0.0004$, $p = 0.95$	Path = 4.26–0.002*AUC $r^2(14) = 0.012$, $p = 0.69$	Path = 4.2–0.002*AUC $r^2(14) = 0.02$, $p = 0.61$

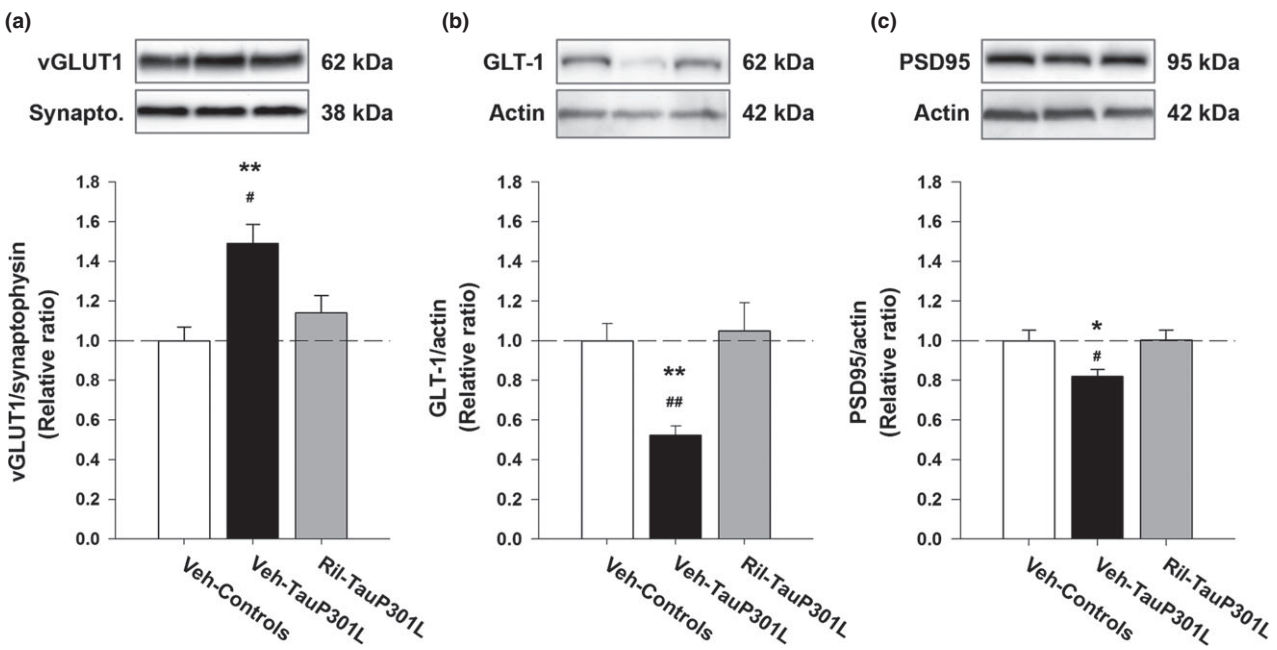

Fig. 6 Riluzole rectifies alterations in tripartite synapse associated with P301L tau expression. (a) Riluzole treatment rescued the P301L-mediated increase in vGLUT1 expression observed in TauP301L mice. (b) Riluzole increased glutamate transporter 1 (GLT-1) expression in TauP301L mice. (c) PSD-95 expression was increased in riluzole-treated TauP301L mice. (Mean ± SEM; $^{*}p < 0.05$ Veh-Controls vs. Veh-TauP301L, $^{**}p < 0.01$ Veh-Controls vs. Veh-TauP301L, $^{\#}p < 0.05$ Ril-TauP301L vs.Veh-TauP301L, $^{\#\#}p < 0.01$ Ril-TauP301L vs.Veh-TauP301L; $n = 12$–14/group).

hyperphosphorylated at residue S202 (CP-13) and the conformational epitope (7–9 and 326–330 aa) recognized by MC-1 (Fig. 7a and b). Similar results were obtained after staining for PHF-1, which recognizes phosphorylation at residue S396/404 [$F(2, 33) = 99.98$, $p < 0.0001$; Fig. 7c]. In addition, detection of total tau (human and mouse) with the Tau-5 antibody revealed a significant reduction in total tau levels in the hippocampus following riluzole treatment [$F(2, 35) = 42.37$, $p < 0.0001$; Fig. 7d]. To examine the activity of glycogen synthase kinase 3 beta (GSK3β), a kinase that phosphorylates tau (Wang *et al.* 1998), we measured Ser9-phosphorylated GSK3β. While expression of GSK3β did not differ among the groups [$F(2, 33) = 0.48$, $p = 0.62$], Veh-TauP301L mice exhibited the decreased phosphorylation at Ser9 [$F(2, 33) = 10.63$, $p = 0.0003$; Fig. 7e], indicating increased GSK3β activity. Riluzole treatment increased Ser9 phosphorylation levels to that of Veh-Controls.

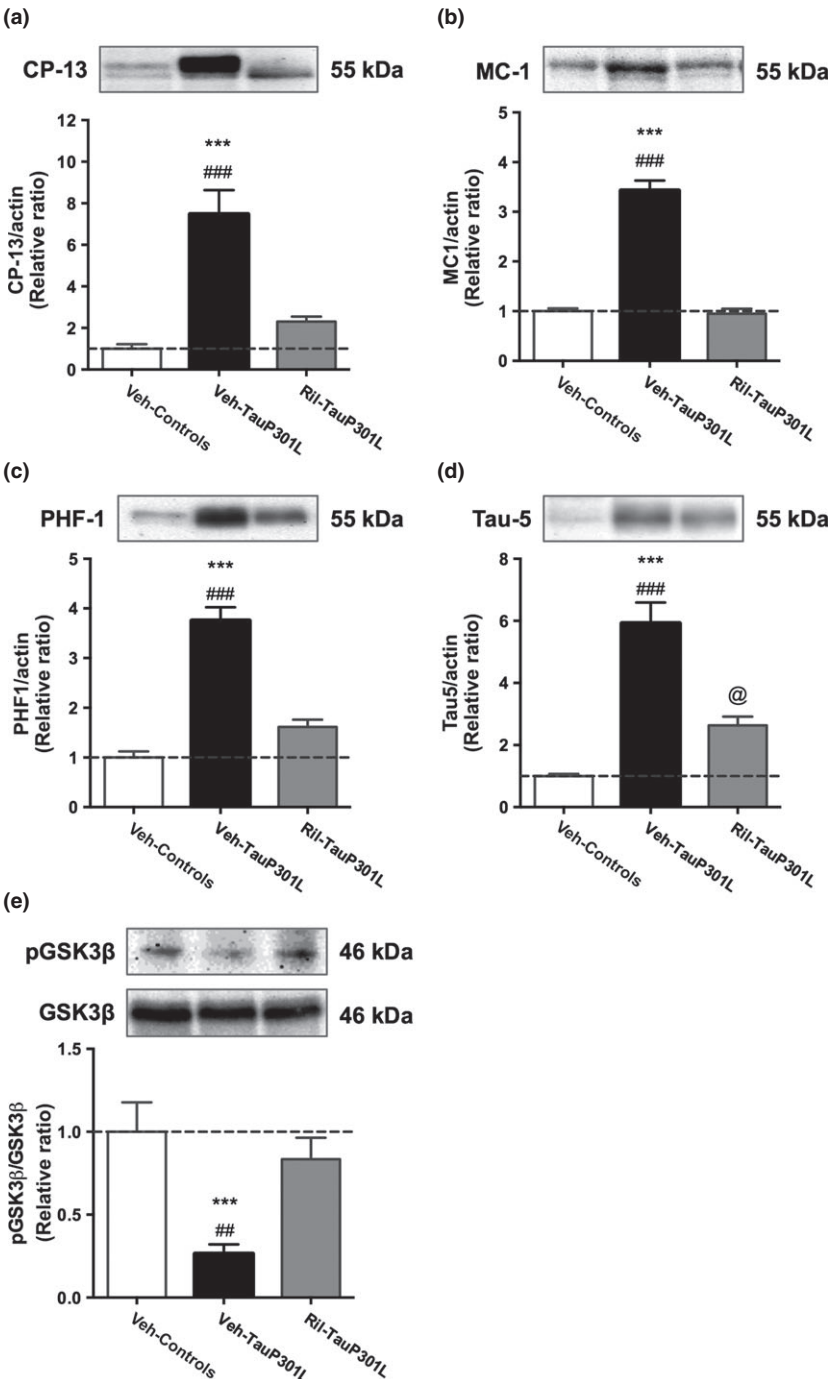

Fig. 7 Riluzole rescues tau pathology. Treating mice with riluzole reduced tau phosphorylation at S202 (a), tau conformational changes (b), phosphorylation at S396/404 (c), and GSK3β activity (e) to control levels. Total tau levels were also significantly reduced by riluzole (d). (Mean ± SEM; $^{***}p < 0.001$ Veh-Controls vs. Veh-TauP301L, $^{\#\#}p < 0.01$ Ril-TauP301L vs.Veh-TauP301L, $^{\#\#\#}p < 0.01$ Ril-TauP301L vs.Veh-TauP301L; $@p < 0.5$ Veh-Controls vs. Ril-TauP301L; n = 12–14/group).

Discussion

Recent work suggests tau may mediate hyperexcitability. For example, deletion of tau in models of epilepsy reduces hyperexcitability, seizure frequency, and duration (DeVos *et al.* 2013; Holth *et al.* 2013). Seizure severity is also reduced in tau knockout mice following convulsant administration (Roberson *et al.* 2007; Ittner *et al.* 2010). Although the exact mechanism remains to be determined, our current findings add to a body of literature suggesting that tau influences hyperexcitability through its effects on glutamate neurotransmission (Roberson *et al.* 2007; Roberson *et al.*, 2011; Hunsberger *et al.* 2014a). Here, we also present evidence that rectifying alterations in glutamatergic circuits can rescue cognitive deficits and tau pathology associated with P301L tau expression.

Although the effects of riluzole on extracellular glutamate have been examined *in vivo* using microdialysis (e.g., Kwon *et al.* 1998), this is the first report of riluzole's effects on the rapid time dynamics of extracellular glutamate as measured by *in vivo* amperometry, which has many benefits over other *in vivo* or *ex vivo* methods. For example, with studies employing microdialysis to measure glutamate, there are often spatial and temporal limitations that restrict the ability to sample dynamic changes in glutamate near the synapse (Obrenovitch *et al.* 2000; Hillered *et al.* 2005). Damage caused by the large sampling area (1–4 mm in length) limits the detection of calcium and sodium dependent neuronal release (Borland *et al.* 2005; Jaquins-Gerstl and Michael 2009), and the low temporal resolution (1–20 min) is inadequate to measure the fast dynamics of transient release and uptake of glutamate (Diamond 2005). The MEAs allow for such measures because of their high temporal resolution (2 Hz), low limit of detection (< 0.5 μM), and high spatial resolution, allowing for selective measurement of extracellular glutamate closer to synapses (Burmeister and Gerhardt 2001; Burmeister *et al.* 2002; Rutherford *et al.* 2007; Hascup *et al.* 2010). Another benefit of MEAs over other *ex vivo* methods is the ability to study brain regions *in vivo* without disrupting their extrinsic and intrinsic connections, a particularly important consideration when examining the complex neural networks of the hippocampus. An important consideration for future studies includes the examination of the effects of riluzole per se in wild-type littermate controls, a limitation of the current design.

Using this technique, we observed increases in both tonic and evoked glutamate release and decreases in glutamate uptake in TauP301L mice. Riluzole treatment appeared to return these shifts in glutamate regulation to control levels. *In vitro* studies support that a major portion of tonic glutamate is mediated by glia-dependent release of glutamate, and not vesicular glutamate release (Jabaudon *et al.* 1999; Cavelier and Attwell 2005; Le Meur *et al.* 2007). However, our MEAs appear to measure resting glutamate levels that are diminished by ~ 50% by inhibitors of calcium and sodium channels (Hascup *et al.* 2010), supporting that resting glutamate has a major neuronal component. Similarly, local application of DL-threo-beta-benzyloxyaspartate TBOA to inhibit glutamate transporters leads to an increase in tonic glutamate levels, suggesting transporters also help maintain normal tonic glutamate levels (Day *et al.* 2006; Hascup *et al.* 2010). Delineation of the possible mechanisms mediating the increase tonic levels in TauP301L mice will be carried out in future studies. Interestingly, in our previous work (Hunsberger *et al.* 2014a), we did not observe differences in tonic (resting) glutamate levels between Controls and TauP301L mice. However, in this study, TauP301L mice exhibited increased levels of tonic glutamate, particularly in the CA3 and CA1 regions. This difference in findings between studies may be because of the duration of tau expression at the time of testing. In the original study (Hunsberger *et al.* 2014a), mice expressed tau for approximately 3 months, whereas in this study, mice expressed tau for approximately 5 months. Thus, with longer durations of tau expression, tonic glutamate may also become deregulated by P301L tau expression, a hypothesis that warrants further testing.

An interesting phenomenon, observed in both our previous study (Hunsberger *et al.* 2014a) and this study, is the subregional relationships between extracellular glutamate alterations and learning deficits. In both studies, glutamate release in the CA3, but not the DG or CA1, was correlated with performance in learning trials of TauP301L mice, whereas glutamate uptake in the DG and CA1, but not the CA3, was associated with deficits in learning. At this time, we can only speculate as to the reason for these subregional relationships with performance in learning trials, though the circuitry of the hippocampus may offer some clues, particularly for the negative correlation between glutamate release in the CA3 and learning. In the trisynaptic loop of the hippocampus, flow is mainly unidirectional with information entering the loop via the entorhinal cortex with projections running from the DG to the CA3 to the CA1 and back again to the EC. CA3 neurons also receive more than 95% of their input from recurrent CA3 collaterals, referred to as 'auto-associative' tracts. It is these recurrent CA3 collaterals that may make the CA3 particularly susceptible to increases in glutamate release. Support for this comes from studies examining hippocampal activity in cognitively impaired, aged rodents and humans; the CA3 is notably the most hyperexcitable region and this hyperexcitability correlates with cognitive performance (Wilson *et al.* 2005a; Yassa *et al.* 2010; Bakker *et al.* 2012). Reducing CA3 hyperactivity improves memory in aged rats (Koh *et al.* 2010). Examination of the effects of subregional manipulations of glutamatergic activity on cognitive performance will help address these issues, as will studies examining the temporal relations of these circuits with aging and longer durations of P301L tau expression.

In this study, we also examined the relation between extracellular glutamate alterations and memory using performance in probe trials (PCI). Whereas hidden platform acquisition is considered to measure hippocampus-dependent learning, probe trial performance is considered to measure spatial reference memory or strength of spatial memory (Lipp and Wolfer 1998; Jeltsch *et al.* 2001). Surprisingly, only tonic glutamate in the DG, CA3, and CA1 correlated with memory deficits; neither KCl-evoked release nor glutamate uptake predicted memory performance. This lack of relation with memory deficits is surprising given the consistent relations among glutamate measures and the learning deficits observed during acquisition of the MWM (pathlength) in this study (Table 1) and the Barnes maze (errors) in our previous study (Hunsberger *et al.* 2014a). The reason for the discrepancies in learning and memory relations remains unclear at this time, though work by others suggest other hippocampal alterations, such as hippocampal neurogenesis, correlate with acquisition during hidden platform trials, but not probe trial performance, in the MWM (Kempermann and Gage 2002). Because most researchers run correlations with probe performance measures, and not measures of learning or acquisition, these differential relations may be more common than a search of the literature suggests. Further examination and delineation of these relations is warranted.

Increased hippocampal activation in mild cognitive impairment is predictive of the degree and rate of cognitive decline, as well as the conversion to AD (Mackenzie and Miller 1994). Recent work sheds light on one way in which hyperactivity might be permissive for the development of AD. In AD, tau – typically an intracellular protein – is released into the extracellular space and endocytosed by neighboring neurons (Liu *et al.* 2012). This spread occurs along synaptically connected circuits, resulting in a prion-like cell-to-cell transmission of tau pathology. Relevant to this study is the finding that glutamate release and stimulation of glutamate receptors induces tau release from neurons into the extracellular space (Pooler *et al.* 2013; Yamada *et al.* 2014). Thus, glutamate-mediated exocytosis of tau may indicate one mechanism for the trans-synaptic spread of tau pathology associated with synaptic activity. This could also result in a vicious feed-forward cycle whereby tau pathology increases glutamate signaling, which then propagates the spread of tau pathology. Prevention of this spread may be one means by which riluzole treatment reduced total tau levels. Further studies are needed to establish the relevance of increased glutamate signaling to the spread of tau pathology.

Acknowledgments and conflict of interest disclosure

This work was supported by the National Institute of General Medical Sciences (Reed - U54GM104942), NIA (Reed - R15AG045812), the Alzheimer's Association (Reed - NIRG-12-242187), a WVU Faculty Research Senate Grant, and a WVU PSCOR grant. GG is the sole proprietor of Quanteon, LLC that makes the Fast-16 recording system used for glutamate measurements in this study.

All experiments were conducted in compliance with the ARRIVE guidelines.

Supporting information

Additional supporting information may be found in the online version of this article at the publisher's web-site:

Figure S1. Prior to tau expression and riluzole treatment, there were no differences among the groups for reference memory errors (a), working memory incorrect errors (b), and working correct errors (c) during acquisition or delay trials (d) in the water radial arm maze.

Figure S2. Males made more reference memory errors (a), working memory incorrect errors (b), and working correct errors (c) during acquisition of the water radial arm maze at 5 months of age.

Figure S3. There were no differences among the groups for reference memory errors (a and d), working memory incorrect errors (b and e), and working correct errors (c and f) during acquisition in the water radial arm maze at 5 and 7.5 months of age, respectively.

Figure S4. There were no differences among the groups for reference memory errors, working memory incorrect errors, and working correct errors during delay trials at 5 months of age (a) and 7.5 months of age (b).

Figure S5. Swim speeds at 5 months of age (a) and 7.5 months of age (b) were similar among the groups.

References

Azbill R. D., Mu X. and Springer J. E. (2000) Riluzole increases high-affinity glutamate uptake in rat spinal cord synaptosomes. *Brain Res.* **871**, 175–180.

Bakker A., Krauss Gregory. L., Albert Marilyn. S. *et al.* (2012) Reduction of hippocampal hyperactivity improves cognition in amnestic mild cognitive impairment. *Neuron* **74**, 467–474.

Bassett S. S., Yousem D. M., Cristinzio C., Kusevic I., Yassa M. A., Caffo B. S. and Zeger S. L. (2006) Familial risk for Alzheimer's disease alters fMRI activation patterns. *Brain* **129**, 1229–1239.

Bimonte-Nelson H. A., Hunter C. L., Nelson M. E. and Granholm A. C. (2003) Frontal cortex BDNF levels correlate with working memory in an animal model of Down syndrome. *Behav. Brain Res.* **139**, 47–57.

Bondi M. W., Houston W. S., Eyler L. T. and Brown G. G. (2005) fMRI evidence of compensatory mechanisms in older adults at genetic risk for Alzheimer disease. *Neurology* **64**, 501–508.

Bookheimer S. Y., Strojwas M. H., Cohen M. S., Saunders A. M., Pericak-Vance M. A., Mazziotta J. C. and Small G. W. (2000) Patterns of brain activation in people at risk for Alzheimer's disease. *N. Engl. J. Med.* **343**, 450–456.

Borland L. M., Shi G., Yang H. and Michael A. C. (2005) Voltammetric study of extracellular dopamine near microdialysis probes acutely implanted in the striatum of the anesthetized rat. *J. Neurosci. Methods* **146**, 149–158.

Braak H. and Braak E. (1998) Argyrophilic grain disease: frequency of occurrence in different age categories and neuropathological diagnostic criteria. *J. Neural. Transm.* **105**, 801–819.

Braden B. B., Talboom J. S., Crain I. D., Simard A. R., Lukas R. J., Prokai L., Scheldrup M. R., Bowman B. L. and Bimonte-Nelson H. A. (2010) Medroxyprogesterone acetate impairs memory and alters

the GABAergic system in aged surgically menopausal rats. *Neurobiol. Learn. Mem.* **93**, 444–453.

Brier M. R., Thomas J. B., Snyder A. Z., Benzinger T. L., Zhang D., Raichle M. E., Holtzman D. M., Morris J. C. and Ances B. M. (2012) Loss of intranetwork and internetwork resting state functional connections with Alzheimer's disease progression. *J. Neurosci.* **32**, 8890–8899.

Burmeister J. J. and Gerhardt G. A. (2001) Self-referencing ceramic-based multisite microelectrodes for the detection and elimination of interferences from the measurement of L-glutamate and other analytes. *Anal. Chem.* **73**, 1037–1042.

Burmeister J. J., Pomerleau F., Palmer M., Day B. K., Huettl P. and Gerhardt G. A. (2002) Improved ceramic-based multisite microelectrode for rapid measurements of L-glutamate in the CNS. *J. Neurosci. Methods* **119**, 163–171.

Busche M. A., Eichhoff G., Adelsberger H., Abramowski D., Wiederhold K. H., Haass C., Staufenbiel M., Konnerth A. and Garaschuk O. (2008) Clusters of hyperactive neurons near amyloid plaques in a mouse model of Alzheimer's disease. *Science* **321**, 1686–1689.

Cavelier P. and Attwell D. (2005) Tonic release of glutamate by a DIDS-sensitive mechanism in rat hippocampal slices. *J. Physiol.* **564**, 397–410.

Day B. K., Pomerleau F., Burmeister J. J., Huettl P. and Gerhardt G. A. (2006) Microelectrode array studies of basal and potassium-evoked release of L-glutamate in the anesthetized rat brain. *J. Neurochem.* **96**, 1626–1635. Epub 2006 Jan 1625.

DeVos S. L., Goncharoff D. K., Chen G. *et al.* (2013) Antisense reduction of tau in adult mice protects against seizures. *J. Neurosci.* **33**, 12887–12897.

Diamond J. S. (2005) Deriving the glutamate clearance time course from transporter currents in CA1 hippocampal astrocytes: transmitter uptake gets faster during development. *J. Neurosci.* **25**, 2906–2916.

Du A. T., Schuff N., Kramer J. H. *et al.* (2004) Higher atrophy rate of entorhinal cortex than hippocampus in AD. *Neurology* **62**, 422–427.

Engler-Chiurazzi E., Tsang C., Nonnenmacher S., Liang W. S., Corneveaux J. J., Prokai L., Huentelman M. J. and Bimonte-Nelson H. A. (2011) Tonic Premarin dose-dependently enhances memory, affects neurotrophin protein levels and alters gene expression in middle-aged rats. *Neurobiol. Aging* **32**, 680–697.

Filippini N., MacIntosh B. J., Hough M. G., Goodwin G. M., Frisoni G. B., Smith S. M., Matthews P. M., Beckmann C. F. and Mackay C. E. (2009) Distinct patterns of brain activity in young carriers of the APOE-epsilon4 allele. *Proc. Natl Acad. Sci. USA* **106**, 7209–7214.

Friedemann M. N. and Gerhardt G. A. (1992) Regional effects of aging on dopaminergic function in the Fischer-344 rat. *Neurobiol. Aging* **13**, 325–332.

Frizzo M. E., Dall'Onder L. P., Dalcin K. B. and Souza D. O. (2004) Riluzole enhances glutamate uptake in rat astrocyte cultures. *Cell. Mol. Neurobiol.* **24**, 123–128.

Fumagalli E., Funicello M., Rauen T., Gobbi M. and Mennini T. (2008) Riluzole enhances the activity of glutamate transporters GLAST, GLT1 and EAAC1. *Eur. J. Pharmacol.* **578**, 171–176. Epub 2007 Oct 25.

Gegelashvili G. and Schousboe A. (1998) Cellular distribution and kinetic properties of high-affinity glutamate transporters. *Brain Res. Bull.* **45**, 233–238.

Gourley S. L., Espitia J. W., Sanacora G. and Taylor J. R. (2012) Antidepressant-like properties of oral riluzole and utility of incentive disengagement models of depression in mice. *Psychopharmacology* **219**, 805–814. Epub 2011 Jul 21.

Greenamyre J. T. and Young A. B. (1989) Excitatory amino acids and Alzheimer's disease. *Neurobiol. Aging* **10**, 593–602.

Greene J. G., Borges K. and Dingledine R. (2009) Quantitative transcriptional neuroanatomy of the rat hippocampus: evidence for wide-ranging, pathway-specific heterogeneity among three principal cell layers. *Hippocampus* **19**, 253–264.

Hascup E. R., af Bjerken S., Hascup K. N., Pomerleau F., Huettl P., Stromberg I. and Gerhardt G. A. (2009) Histological studies of the effects of chronic implantation of ceramic-based microelectrode arrays and microdialysis probes in rat prefrontal cortex. *Brain Res.* **1291**, 12–20.

Hascup E. R., Hascup K. N., Stephens M., Pomerleau F., Huettl P., Gratton A. and Gerhardt G. A. (2010) Rapid microelectrode measurements and the origin and regulation of extracellular glutamate in rat prefrontal cortex. *J. Neurochem.* **115**, 1608–1620.

Hillered L., Vespa P. M. and Hovda D. A. (2005) Translational neurochemical research in acute human brain injury: the current status and potential future for cerebral microdialysis. *J. Neurotrauma* **22**, 3–41.

Hinzman J. M., Thomas T. C., Burmeister J. J., Quintero J. E., Huettl P., Pomerleau F., Gerhardt G. A. and Lifshitz J. (2010) Diffuse brain injury elevates tonic glutamate levels and potassium-evoked glutamate release in discrete brain regions at two days post-injury: an enzyme-based microelectrode array study. *J. Neurotrauma* **27**, 889–899.

Hinzman J. M., Thomas T. C., Quintero J. E., Gerhardt G. A. and Lifshitz J. (2012) Disruptions in the regulation of extracellular glutamate by neurons and glia in the rat striatum two days after diffuse brain injury. *J. Neurotrauma* **29**, 1197–1208.

Hölscher C. (1999) Stress impairs performance in spatial water maze learning tasks. *Behav. Brain Res.* **100**, 225–235.

Holth J. K., Bomben V. C., Reed J. G., Inoue T., Younkin L., Younkin S. G., Pautler R. G., Botas J. and Noebels J. L. (2013) Tau loss attenuates neuronal network hyperexcitability in mouse and Drosophila genetic models of epilepsy. *J. Neurosci.* **33**, 1651–1659.

Hunsberger H., Rudy C., Batten S., Gerhardt G. and Reed M. (2014a) P301L tau expression affects glutamate release and clearance in the hippocampal trisynaptic pathway. *J. Neurochem.* **32**, 169–8.

Hunsberger H., Rudy C., Weitzner D., Zhang C., Tosto D., Knowlan K., Xu Y. and Reed M. (2014b) Effect size of memory deficits in mice with adult-onset P301L tau expression. *Behav. Brain Res.* **272**, 181–195.

Ishiyama T., Okada R., Nishibe H., Mitsumoto H. and Nakayama C. (2004) Riluzole slows the progression of neuromuscular dysfunction in the wobbler mouse motor neuron disease. *Brain Res.* **1019**, 226–236.

Ittner L. M., Ke Y. D., Delerue F. *et al.* (2010) Dendritic function of tau mediates amyloid-[beta] toxicity in Alzheimer's disease mouse models. *Cell* **142**, 387–397.

Jabaudon D., Shimamoto K., Yasuda-Kamatani Y., Scanziani M., Gahwiler B. H. and Gerber U. (1999) Inhibition of uptake unmasks rapid extracellular turnover of glutamate of nonvesicular origin. *Proc. Natl Acad. Sci. USA* **96**, 8733–8738.

Jaquins-Gerstl A. and Michael A. C. (2009) Comparison of the brain penetration injury associated with microdialysis and voltammetry. *J. Neurosci. Methods* **183**, 127–135.

Jeltsch H., Bertrand F., Lazarus C. and Cassel J.-C. (2001) Cognitive Performances and Locomotor Activity Following Dentate Granule Cell Damage in Rats: role of Lesion Extent and Type of Memory Tested. *Neurobiol. Learn. Mem.* **76**, 81–105.

Kamenetz F., Tomita T., Hsieh H., Seabrook G., Borchelt D., Iwatsubo T., Sisodia S. and Malinow R. (2003) APP processing and synaptic function. *Neuron* **37**, 925–937.

Kempermann G. and Gage F. H. (2002) Genetic determinants of adult hippocampal neurogenesis correlate with acquisition, but not probe trial performance, in the water maze task. *Eur. J. Neurosci.* **16**, 129–136.

Koh M. T., Haberman R. P., Foti S., McCown T. J. and Gallagher M. (2010) Treatment strategies targeting excess hippocampal activity benefit aged rats with cognitive impairment. *Neuropsychopharmacology* **35**, 1016–1025.

Kwon J. Y., Bacher A. and Zornow M. H. (1998) Riluzole does not attenuate increases in hippocampal glutamate concentrations in a rabbit model of repeated transient global cerebral ischemia. *Anesth. Analg.* **86**, 128–133.

Le Meur K., Galante M., Angulo M. C. and Audinat E. (2007) Tonic activation of NMDA receptors by ambient glutamate of non-synaptic origin in the rat hippocampus. *J. Physiol.* **580**, 373–383.

Lipp H. P. and Wolfer D. P. (1998) Genetically modified mice and cognition. *Curr. Opin. Neurobiol.* **8**, 272–280.

Liu L., Drouet V., Wu J. W., Witter M. P., Small S. A., Clelland C. and Duff K. (2012) Trans-synaptic spread of tau pathology in vivo. *PLoS ONE* **7**, e31302.

Mackenzie I. R. and Miller L. A. (1994) Senile plaques in temporal lobe epilepsy. *Acta Neuropathol.* **87**, 504–510.

Miller R. G., Mitchell J. D., Lyon M. and Moore D. H. (2003) Riluzole for amyotrophic lateral sclerosis (ALS)/motor neuron disease (MND). *Amyotroph. Lateral Scler. Other Motor Neuron Disord.* **4**, 191–206.

Nickell J., Salvatore M. F., Pomerleau F., Apparsundaram S. and Gerhardt G. A. (2007) Reduced plasma membrane surface expression of GLAST mediates decreased glutamate regulation in the aged striatum. *Neurobiol. Aging* **28**, 1737–1748.

Obrenovitch T. P., Urenjak J., Zilkha E. and Jay T. M. (2000) Excitotoxicity in neurological disorders–the glutamate paradox. *Int. J. Dev. Neurosci.* **18**, 281–287.

Palop J. J., Chin J. and Mucke L. (2006) A network dysfunction perspective on neurodegenerative diseases. *Nature* **443**, 768–773.

Paxinos G. and Franklin K. (2012) *Mouse Brain in Stereotaxic Coordinates*. Academic Press, Waltham, Massachusetts.

Paulson J. B., Ramsden M., Forster C., Sherman M. A., McGowan E. and Ashe K. H. (2008) Amyloid plaque and neurofibrillary tangle pathology in a regulatable mouse model of Alzheimer's disease. *Am. J. Pathol.* **173**, 762–772.

Pittenger C., Coric V., Banasr M., Bloch M., Krystal J. H. and Sanacora G. (2008) Riluzole in the treatment of mood and anxiety disorders. *CNS Drugs* **22**, 761–786.

van de Pol L. A., van der Flier W. M., Korf E. S., Fox N. C., Barkhof F. and Scheltens P. (2007) Baseline predictors of rates of hippocampal atrophy in mild cognitive impairment. *Neurology* **69**, 1491–1497.

Pooler A. M., Phillips E. C., Lau D. H., Noble W. and Hanger D. P. (2013) Physiological release of endogenous tau is stimulated by neuronal activity. *EMBO Rep.* **14**, 389–394.

Quiroz Y. T., Budson A. E., Celone K., Ruiz A., Newmark R., Castrillon G., Lopera F. and Stern C. E. (2010) Hippocampal hyperactivation in presymptomatic familial Alzheimer's disease. *Ann. Neurol.* **68**, 865–875.

Roberson E. D., Scearce-Levie K., Palop J. J., Yan F., Cheng I. H., Wu T., Gerstein H., Yu G. Q. and Mucke L. (2007) Reducing endogenous tau ameliorates amyloid beta-induced deficits in an Alzheimer's disease mouse model. *Science* **316**, 750–754.

Roberson E. D., Halabisky B., Yoo J. W. *et al.* (2011) Amyloid-beta/Fyn-induced synaptic, network, and cognitive impairments depend on tau levels in multiple mouse models of Alzheimer's disease. *J. Neurosci.* **31**, 700–711.

Rutherford E. C., Pomerleau F., Huettl P., Stromberg I. and Gerhardt G. A. (2007) Chronic second-by-second measures of L-glutamate in the central nervous system of freely moving rats. *J. Neurochem.* **102**, 712–722.

SantaCruz K., Lewis J., Spires T. *et al.* (2005) Tau suppression in a neurodegenerative mouse model improves memory function. *Science* **309**, 476–481.

Sperling R. A., Dickerson B. C., Pihlajamaki M. *et al.* (2010) Functional alterations in memory networks in early Alzheimer's disease. *Neuromolecular Med.* **12**, 27–43.

Sykova E., Mazel T. and Simonova Z. (1998) Diffusion constraints and neuron-glia interaction during aging. *Exp. Gerontol.* **33**, 837–851.

Vossel K. A., Beagle A. J., Rabinovici G. D. *et al.* (2013) Seizures and epileptiform activity in the early stages of Alzheimer disease. *JAMA Neurol.* **70**, 1158–1166.

Wagner M. L. and Landis B. E. (1997) Riluzole: a new agent for amyotrophic lateral sclerosis. *Ann. Pharmacother.* **31**, 738–744.

Wang J. Z., Wu Q., Smith A., Grundke-Iqbal I. and Iqbal K. (1998) Tau is phosphorylated by GSK-3 at several sites found in Alzheimer disease and its biological activity markedly inhibited only after it is prephosphorylated by A-kinase. *FEBS Lett.* **436**, 28–34.

Wilson I. A., Ikonen S., Gallagher M., Eichenbaum H. and Tanila H. (2005a) Age-associated alterations of hippocampal place cells are subregion specific. *J. Neurosci.* **25**, 6877–6886.

Wilson N. R., Kang J., Hueske E. V., Leung T., Varoqui H., Murnick J. G., Erickson J. D. and Liu G. (2005b) Presynaptic regulation of quantal size by the vesicular glutamate transporter VGLUT1. *J. Neurosci.* **25**, 6221–6234.

Yamada K., Holth J. K., Liao F. *et al.* (2014) Neuronal activity regulates extracellular tau in vivo. *J. Exp. Med.* **211**, 387–393.

Yassa M. A., Stark S. M., Bakker A., Albert M. S., Gallagher M. and Stark C. E. L. (2010) High-resolution structural and functional MRI of hippocampal CA3 and dentate gyrus in patients with amnestic Mild Cognitive Impairment. *NeuroImage* **51**, 1242–1252.

Zhang H. T., Huang Y., Masood A. *et al.* (2008) Anxiogenic-like behavioral phenotype of mice deficient in phosphodiesterase 4B (PDE4B). *Neuropsychopharmacology* **33**, 1611–1623.